

Thermal analysis for brake disks of SiC/6061 Al alloy co-continuous composite for CRH3 during emergency braking considering airflow cooling

JIANG Lan¹, JIANG Yan-li², YU Liang², SU Nan¹, DING You-dong¹

1. School of Materials and Metallurgy, Northeastern University, Shenyang 110819, China;

2. Key Laboratory of New Processing Technology for Nonferrous Metals and Materials, Ministry of Education, Guilin University of Technology, Guilin 543004, China

Received 23 September 2011; accepted 5 January 2011

Abstract: The mass of high-speed trains can be reduced using the brake disk prepared with SiC network ceramic frame reinforced 6061 aluminum alloy composite (SiC_n/Al). The thermal and stress analyses of SiC_n/Al brake disk during emergency braking at a speed of 300 km/h considering airflow cooling were investigated using finite element (FE) and computational fluid dynamics (CFD) methods. All three modes of heat transfer (conduction, convection and radiation) were analyzed along with the design features of the brake assembly and their interfaces. The results suggested that the higher convection coefficients achieved with airflow cooling will not only reduce the maximum temperature in the braking but also reduce the thermal gradients, since heat will be removed faster from hotter parts of the disk. Airflow cooling should be effective to reduce the risk of hot spot formation and disc thermal distortion. The highest temperature after emergency braking was 461 °C and 359 °C without and with considering airflow cooling, respectively. The equivalent stress could reach 269 MPa and 164 MPa without and with considering airflow cooling, respectively. However, the maximum surface stress may exceed the material yield strength during an emergency braking, which may cause a plastic damage accumulation in a brake disk without cooling. The simulation results are consistent with the experimental results well.

Key words: finite element method; brake disk; co-continuous SiC/6061 composite; thermal analysis; airflow cool

1 Introduction

Lightweight is one of the key technologies for the high-speed trains. Unsprung weight can be reduced by using SiC/Al brake disk, so as to reduce the weight of high-speed trains. Comparing to iron and steels, SiC/Al composite has larger linear expansion coefficient and lower strength at high temperature, which increases the thermal damage tendency and limits the speed range of SiC/Al brake disks [1]. Recently, the co-continuous metal–ceramic composites have been applied widely to dry friction and wear applications since they can effectively enhance the tribological performance of the materials [2,3]. Since the SiC continuous network structure ceramics are a very promising material for high temperature structural applications and reinforcement in the SiC/6061 alloy composite materials, the composites have excellent mechanical properties and friction

behavior, and can be used as the brake disk material [4,5]. In our previous work, the co-continuous SiC/Al alloy composites (SiC_n/Al) consisting of two interpenetrating continuous networks, Al alloy and SiC ceramic, were prepared [5,6]. It is well known that the main problem of braking and stopping a high-speed train, such as China Railway High-speed 3 (CRH3) system, is the great input of heat flux into the disk in a very short time. High temperature can cause a fall in friction coefficient, or fade, and increased wear of both discs and pads [7]. Both fade and increased wear are affected by local thermal distortions of the disc, which can lead to macroscopic hot spots (MHS) [8]. These MHSs are amongst the most dangerous phenomena in brakes, since they are associated with high thermal gradients. The consequent stress fields can lead to low cycle fatigue of the discs, cracking, and even catastrophic failure [9]. For these reasons, brake discs are often designed with slots or holes to create turbulence as they rotate, and thus to

Foundation item: Projects (50872018, 50902018) supported by the National Natural Science Foundation of China; Project (1099043) supported by the Science and Technology in Guangxi Province, China; Project (090302005) supported by the Basic Research Fund for Northeastern University, China

Corresponding author: JIANG Lan; Tel: +86-24-83681325; E-mail: jiangl@smm.neu.edu.cn

DOI: 10.1016/S1003-6326(11)61533-1

enhance convective heat transfer to the air [10]. The design constraints on the discs make it difficult to optimize every aspect of their design simultaneously, since it is desirable to optimize the weight and stiffness of the discs as well as their heat capacity and heat transfer capability, which leads to conflicting design requirements. The methods solving brake disk optimization concentrated on finite element method [11,12], approximate integration method [13,14], Green's function method [15] and Laplace transformation method [16], etc. The former three methods are numerical solution methods and are of low relative accuracy. For example, finite element method can solve the complicate heat conduction problem, but the accuracy of computational solution is relatively low, which is affected by mesh density, step length and so on. Though the Laplace transformation method is an analytic solution method, it is difficult to solve the equation of heat conduction with complicated boundaries. In fact, the temperature gradient and thermal stress of the brake disk are affected by the airflow through and around it. However, seldom calculations consider cooling with wind during the braking process. Therefore, the analytic solution called finite element (FE) and computational fluid dynamics (CFD) methods was adopted [17], because it is suitable for solving the problem of non-homogeneous transient heat conduction with airflow cooling.

This work was focused on the temperature and thermal stress analysis of the co-continuous $\text{SiC}_n/6061 \text{ Al}$ alloy composite ($\text{SiC}_n/6061 \text{ Al}$) brake disk of CRH3 under centrifugal and thermal load during emergency braking considering airflow cooling, with the help of finite element calculation software. The airflow through and around the brake disk was analyzed [18]. The multi-contact elastic-plastic thermal-mechanical coupling model of disc brake was established in order to investigate the thermal-mechanical coupling problems. This provides the methods for the research on the thermal damage and structural design of the brake disk. The heat transfer coefficients considering convection and radiation were calculated and later used as a boundary condition in thermal numerical analysis using the Solidwork2012 Flow software package [19].

2 Modeling for calculation

The $\text{SiC}_n/6061 \text{ Al}$ composite was obtained by infiltration of molten 6061 Al alloy (0.40%–0.80% Si, 0.70% Fe, 0.15%–0.40% Cu, 0.15% Mn, 0.80%–1.20% Mg, 0.04%–0.35% S Cr, 0.25% Zn, 0.15% Ti, balance Al) into SiC network ceramic by vacuum-pressure casting

process [20]. The SiC continuous network structure ceramic preforms were prepared by the porous polyurethane coated with large amounts of aqueous reactant containing $\alpha\text{-SiC}$ power (purity>99%, $d_{50}=1.5 \mu\text{m}$). The microstructure of $\text{SiC}_n/6061 \text{ Al}$ is shown in Fig. 1. The bright phase is the 6061 Al alloy matrix, and the dark phase is the SiC network. The models of the $\text{SiC}_n/6061 \text{ Al}$ brake disk for CRH3 high-speed train are shown in Fig. 2. The white part shown in Fig. 2(a) is the 6061 Al alloy matrix for brake disk. The black parts shown in Fig. 2(b) are $\text{SiC}_n/6061 \text{ Al}$ alloy composites which are embedded in the disk. In this analysis the brake disk without wear model was considered. The basic dimension of the brake disk is shown in Fig. 2(d). The brake disk has 22 cooling vanes equally spaced, which enables the usage of symmetry with a basic angle of 15° .

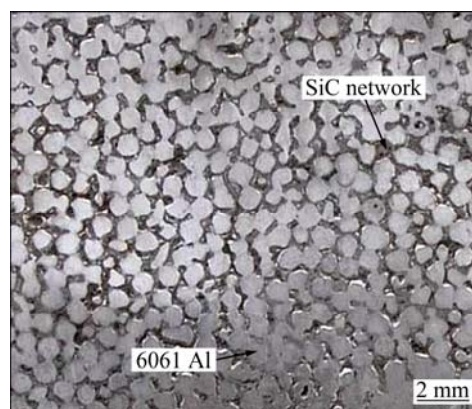


Fig. 1 Microstructure of $\text{SiC}_n/6061 \text{ Al}$ alloy composites

3 Calculation of cooling factors

3.1 Flow calculation boundary

The airflow through and around the brake disk was analyzed using the Solidwork2012 simulation software package. The heat transfer coefficients considering convection and radiation were calculated and organized in such a way that they could be used as a boundary condition in thermal analysis. The averaged heat transfer coefficients at a flow rate of 7.85 L/s, and an angle of 90° , for the nozzle-to-plate spacing H/D values of 3, 6 and 10 were applied in the calculation [21]. The brake disk model for calculation is shown in Fig. 3. A three dimensional model of the whole was chosen for airflow cooling numerical calculation, with size of 1200 mm \times 1200 mm \times 500 mm. The axisymmetric eight-node isoparametric elements were used for the finite element analysis of the model. To allow the gradient of the variables at the interfaces and boundaries, the finer mesh near the interfaces of disk brakes was adopted using the mapping function. The rest of the model was more

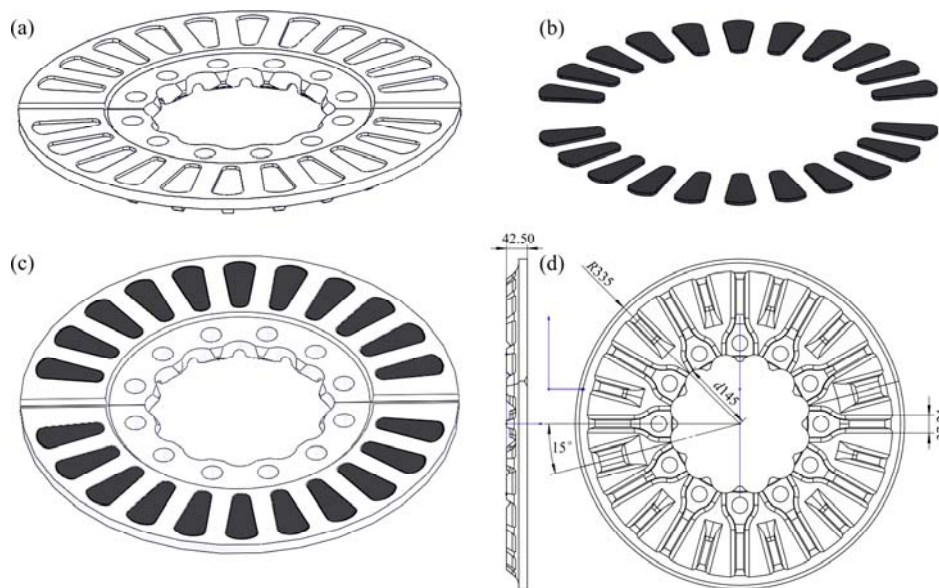


Fig. 2 SiC_n/6061 Al embedded in brake disk for high-speed train: (a) 6061 Al alloy matrix for brake disk; (b) SiC_n/6061 alloy composites array; (c) SiC_n/6061 Al alloy brake disk; (d) Basic geometry of section of brake disk

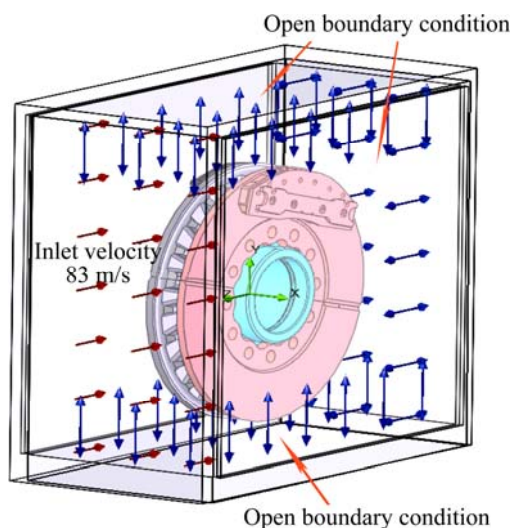


Fig. 3 Boundary conditions for airflow cooling analysis

roughly meshed, as it serves only for inflowing and outflowing air visualization.

The model applied periodic boundary conditions on the section sides. As the brake disk was made out of the SiC_n/6061 Al alloy composite, the surface roughness was taken to be 5 mm. The disk interfaces were heated uniformly. The disk model was attached to an adiabatic shaft whose axial length spans that of the domain. Airflow around the disk was considered to be 30 °C, and open boundaries with zero relative pressure were used for the upper, lower and radial ends of the domain. For modeling the emergency braking phenomena, the brake disk was accelerated with the constant value of 0.8 m/s² and reached the velocity of 300 km/h, then the braking started and caused constant deceleration with the rate of 1.117 m/s² applying emergency braking. During braking,

braking disk temperatures were calculated and used for the numerical simulation considering airflow cooling. Material data were taken from Solidworks Simulation Flow material data library in air at 25 °C. Reference pressure was set to be 1.01×10⁵ Pa, turbulence intensity was low and the turbulent model used for the finite element analysis was *k-ε*.

The Solidwork2012 Flow software package automatically calculates the heat transfer coefficient at the wall boundary using

$$h_c = \frac{q_w}{T_b - T_{nw}} \quad (1)$$

where h_c is the heat transfer coefficient, q_w is the heat flux at the wall boundary, T_b is the boundary temperature (that is, outside the fluid domain) and T_{nw} is the temperature at the internal near-wall boundary element center node [22]. To enable universal usage of the results, the solver had to be set to compute the convective heat transfer coefficient related to ambient (constant) temperature using

$$h_c = \frac{q_w}{T_b - T_\infty} \quad (2)$$

where T_∞ is constant ambient temperature.

The result was converged with approximately 130 iterations, which indicates that the mesh and boundary conditions were properly chosen.

3.2 Thermal calculation boundary

3.2.1 Determination of heat flux load

The brake disc is symmetric, however, the whole disk was modeled in the simulation in order to obtain the relatively accurate calculation results. Temperature

dependent material data were taken from our experiment data and some basic vehicle data are listed in Tables 1 and 2 [23].

Table 1 Properties of brake disks of SiC_n/6061 Al composite

| Property | Value |
|---|------------------|
| Heat conductivity, $\lambda/(\text{W}\cdot\text{m}^{-1}\cdot\text{K}^{-1})$ | 5 |
| Density, $\rho/(\text{kg}\cdot\text{m}^{-3})$ | 3.7×10^3 |
| Specific heat capacity, $c_p/(\text{J}\cdot\text{kg}^{-1}\cdot\text{K}^{-1})$ | 650 |
| Module of elasticity, E/GPa | 254 |
| Poisson number, ν | 0.13 |

Table 2 Basic data for brake disks

| Parameter | Value |
|--|------------------|
| Mass of vehicle, M/kg | 5.5×10^4 |
| Start velocity, $v_0/(\text{m}\cdot\text{s}^{-1})$ | 83 |
| Deceleration, $a/(\text{m}\cdot\text{s}^{-2})$ | 0.77 |
| Braking time, t_b/s | 107 |
| Effective radius of braking disk, r_d/m | 0.254 |
| Radius of wheel, r_w/m | 0.430 |
| Incline of track, $\delta/\%$ | 1.1 |
| Friction coefficient of disk/pad, μ | 0.32 |
| Surface of braking pad, A_c/mm^2 | 2.0×10^4 |

Cooling due to heat convection and radiation was modeled with surface film condition. The film coefficient is dependent upon the part temperature. During each braking, a surface heat flux with the beginning value obtained from Ref. [24] was applied on the interfaces under the brake pads. The heat flux was calculated using basic vehicle data that were available, such as gross vehicle mass, rear/front brake distribution, share of heat taken over by brake disk and basic brake disks geometry. Heat flux is calculated using

$$\dot{Q}(t) = \frac{P_{\text{disc}} - \left(\frac{P_{\text{disc}}}{t_{\text{stop}}} \cdot t\right)}{A_{\text{friction}}} = \begin{cases} 2.7 \text{ W/mm}^2, & t = 0 \text{ s} \\ 0 \text{ W/mm}^2, & t = t_{\text{stop}} \end{cases} \quad (3)$$

where P_{disc} is braking power at each front disk, t_{stop} is the time of braking to standstill, and A_{friction} is the area of the friction ring that the brake pads contact the brake disk.

$$P_{\text{disc}} = \frac{m_{\text{vehicle}} \cdot |a| \cdot d_{f/r} \cdot v_{\text{AMS}} \cdot \eta_{\text{disc}}}{2} \quad (4)$$

The braking power is calculated using Eq. (4). m_{vehicle} is the gross vehicle mass, a is the deceleration, $d_{f/r}$ is the front to rear brake power distribution, v_{AMS} is the initial velocity of braking procedure, and η_{disc} is the share of heat absorbed by brake disk.

As we know the brake pad geometry, it is easy to calculate the area of the friction ring:

$$A_{\text{friction}} = 2\pi(r_0^2 - r_i^2) \quad (5)$$

where r_0 represents the outer diameter of friction ring and r_i is the inner diameter of friction ring. The heat flux has a greatest value at the beginning of braking, then falls linearly to 0 at the end of braking, and remains 0 when the vehicle is accelerating. Another cycle repeats itself when the vehicle is braking again.

3.2.2 Determination of physical model

The goal was to find out the distribution of temperature in the brake disk considering airflow cooling. The initial temperature of the brake disk and the surrounding was 50 °C. The part of the braking energy that transfers to the surrounding air was not considered. The heat flux was applied in the calculation [24]. Additionally, the effect of heat transfer with radiation was considered. Braking on the flat track derives from the physical model for determination of the heat transfer in dependency from the braking time. Besides that, the weight distribution of the vehicle was considered. The weight arrangement was 60/40 [25] in the favor of the front part of the carriage. This means that the front part of the carriage takes 60% of the whole load. In our case only 10% of the whole brake force was applied to one disk from the front part of the carriage. Because of the mentioned weight distribution, only the front part of the carriage was analyzed. Every carriage consists of four axles with three brake disks attached to each axle. The kinetic energy [26] for one wheel considering constant deceleration is

$$\frac{1}{2} M v_0^2 = \int_0^{t_z} P(t) dt = 2 F_{\text{disk}} \int_0^{t_z} v_{\text{disk}}(t) dt \quad (6)$$

The change of energy is equal to the heat flux on the interface of the disk. This ratio was used to calculate the thermal load on the brake disk. Other data used for the analysis are listed in Table 1 and 2.

Force which works on the brake disk is calculated as [27]

$$F_{\text{disk}} = \frac{\frac{1}{2} M v_0^2}{8 \frac{r_d}{r_w} (v_0 t_z - \frac{1}{2} a t_z^2)} = 4235.7 \text{ N} \quad (7)$$

Instant heat flux entering one side of the braking disk is calculated as

$$\begin{aligned} Q(t) &= F_{\text{disk}} \cdot v_{\text{disk}}(t) = F_{\text{disk}} \cdot \frac{r_d}{r_w} \cdot (v_0 - a \cdot t) \\ &= 207667 - 1926 t \text{ W} \end{aligned} \quad (8)$$

The calculated heat flux was considered for both sides of the disk. Because the stress was also analyzed, the disk needs to be properly fixed. The disk was put together rigidly where the disk was screwed onto the hub

as shown in Fig. 4. The forming of the volume mesh was automatic. The mesh consists of 10195 tetrahedral elements. A mesh was created and refined using the mesh refining tool until a sufficient degree of accuracy was reached. To perform the analysis, the material properties from Table 1 and 2 were used.

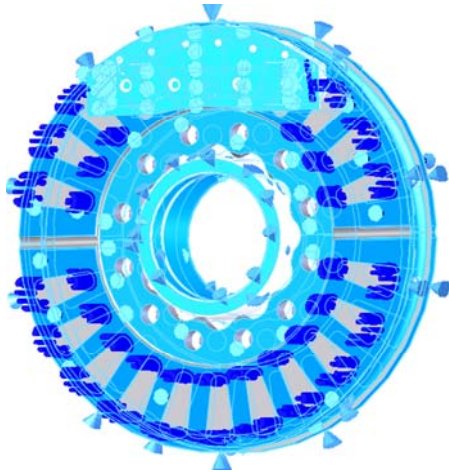


Fig. 4 SiC_n/6061 brake disk section with thermal, force load, and fixing spot

4 Results and discussion

4.1 Flow analysis

The speed of the airflow through the brake disk applying emergency braking with the speed of 300 km/h shown in Fig. 5 have a direct influence on the heat transfer coefficients of the disk as shown in Fig. 6. It can be noticed that where the cooling airflow has a greater velocity, the heat transfer coefficients are higher. For further application of the calculated data in this research, the wall heat transfer coefficients had to be arranged into a form that could be used as an input in the followed thermal simulation.

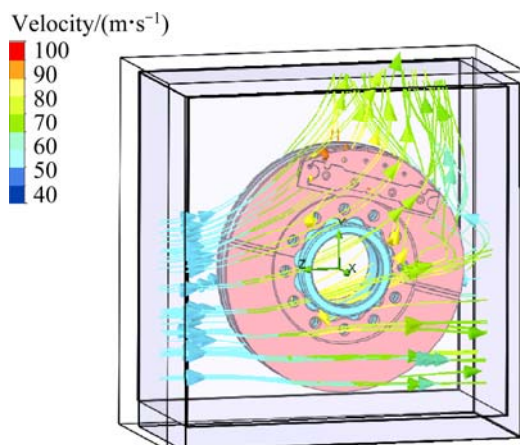


Fig. 5 Speed of airflow through SiC_n/6061 brake disk applying emergency braking with speed of 300 km/h

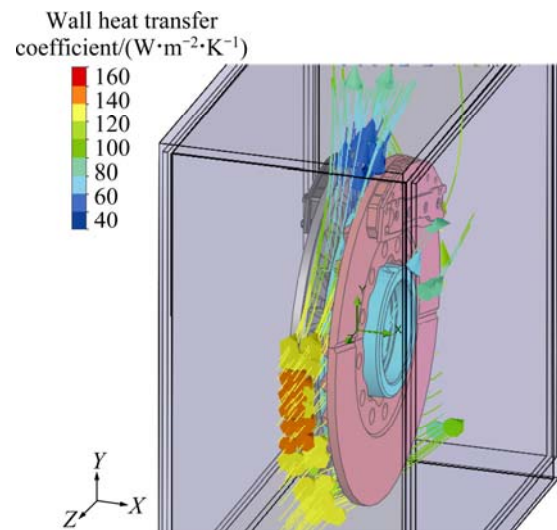


Fig. 6 Heat transfer coefficients of SiC_n/6061 brake disk applying emergency braking with speed of 300 km/h

4.2 Thermal analysis without airflow cooling

The results show that in case of emergency braking on the flat track, the highest temperature in the friction interface of the new SiC_n/6061 disk reaches up to 461 °C without considering airflow cooling, and the highest temperature regions are in the friction ring as shown in Fig. 7(a). The highest allowed temperature of the disk is 600 °C under the long-term condition. In Fig. 7(a), it is noted that the temperature decreases in the direction of median plane of the disk to reach its minimal value. The cooling ribs and the parts where the disk is bolted to the hub are almost unaffected by temperature changing. The higher temperature appears on areas where the wreath of the disk and the cooling ribs are not connected. In this case the ribs are more severely exposed to the heat flux because the disk wreaths are thinner, then the temperature distribution is nonuniform and great temperature gradient exists in a single disc. The maximal temperature is reached after a time period of 107 s, as shown in Fig. 7(b). It is noted that there is an appreciable variation of temperature between the SiC_n/6061 composite and the Al matrix in the disk. The SiC_n/6061 composite can have enhanced thermal performance of energy absorption as compared to the conventional particle-reinforced composites, fiber-reinforced composites, and lamellar composites. According to Figs. 7 and 8, the SiC_n/6061 brake disk has the best thermal behavior.

It is known that the thermal stresses in the disk appear because of the temperature rising. The goal of this analysis is to determine the influence of the centrifugal load and the thermal load. In the case of a flat track and considering the centrifugal load, the stress is given by von Mises stress. The stress is 237 MPa between the disk and pad at the friction interface as shown in Fig. 8(a).

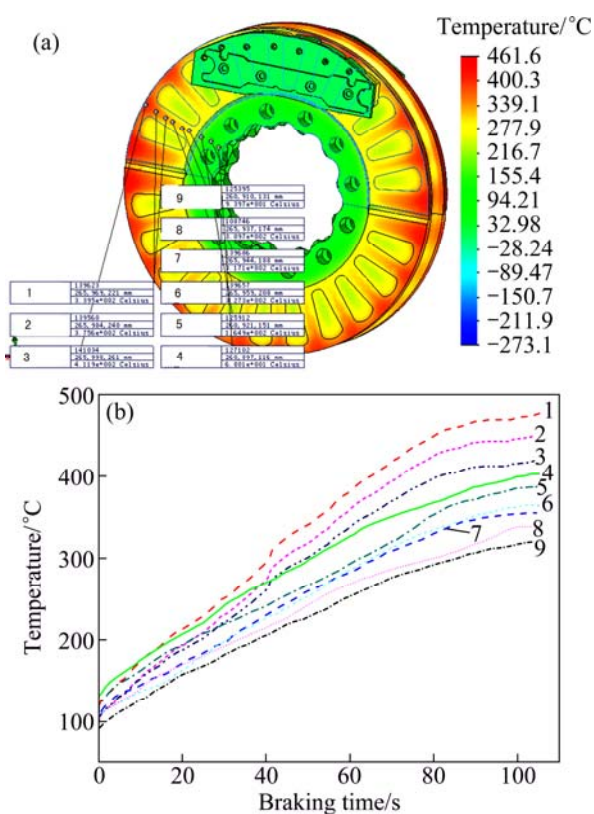


Fig. 7 Temperature distribution of $\text{SiC}_n/6061$ brake disk (a) and temperature plot from beginning to end of simulation (b)

The ribs are more severely exposed to the heat flux because the disk wreaths are thinner, which can lead to the high stress of the disk, where the thermal stress is the highest, 253 MPa, as shown in Fig. 8(b). From the results we can see that on the spots the von Mises stress is 269 MPa, which is still smaller than the permitted value of 314 MPa, considering a safety factor of 1.5. However, the maximum surface stress may exceed the material yield strength during an emergency braking, which may cause a plastic damage accumulation in a brake disk without cooling. From the experimental data it can be concluded that the thermal expansion coefficient and the elastic modulus of the $\text{SiC}_n/6061$ composite have an important effect on the properties of friction surfaces of the brake disk. Consequently, the strain rate dependence is supposed to be well approximated with a bilinear function and the material model strength used was the Johnson-Cook model [28]. From Figs. 8 and 9 it can be observed that the behavior of thermal radial strain is completely different as compared with the behavior of the solid brake disk in Ref. [29]. It can be concluded that the co-continuous microstructure of the $\text{SiC}_n/6061$ composite has significant effect on the thermomechanical response of the disks. In an emergency stop, when most of the kinetic energy of the vehicle is transmitted to the discs as heat, the disc may reach a temperature of 500 °C

[30]. One of the most dangerous conditions in frictional brakes is the formation of MHSs. In this case, we note that the $\text{SiC}_n/6061$ composite will not only reduce the maximum temperature, but also naturally tend to reduce thermal gradients. For the validation purposes of the numerical scheme of the solution, experimental investigations were developed. The results showed that MHSs were explicitly able to be identified, particularly during the emergency braking. And $\text{SiC}_n/6061$ composite might remove heat from the brake disc much more rapidly than the solid Al disc, which may thus provide a means of alleviating some of the thermal problems encountered in practical situations. Theoretical predictions agree well with the experimental estimations.

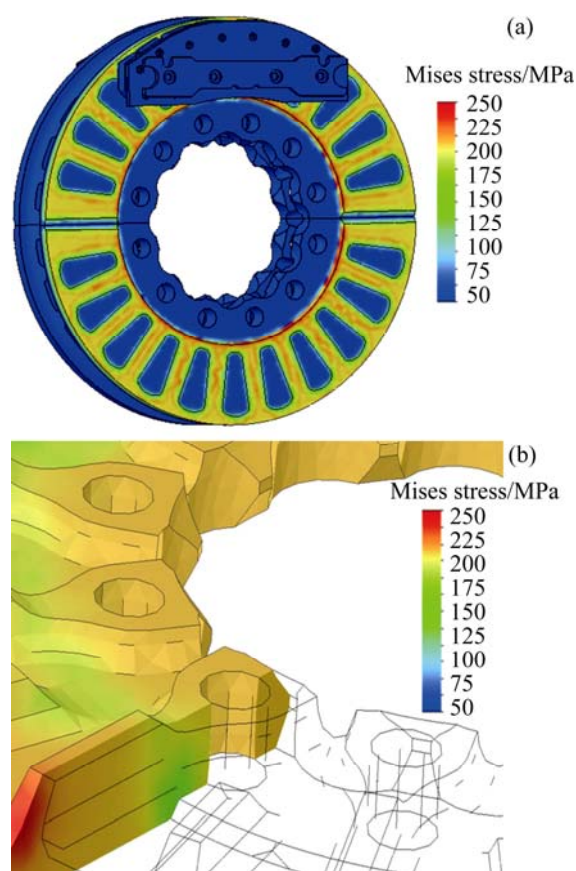


Fig. 8 Numerical simulation of thermal stress of $\text{SiC}_n/6061$ brake disk without considering airflow cooling: (a) Thermal stress distribution of friction interface; (b) Thermal stress distribution from back elevation direction

4.3 Thermal analysis with airflow cooling

4.3.1 Analysis of temperature field

Figure 9(a) shows that in case of emergency braking on the flat track, the highest temperature in the friction interface of the new $\text{SiC}_n/6061$ disk reaches up to 359 °C with considering the airflow cooling. The highest temperature gradient of the friction layer decreases more smoothly along the z -direction, as compared to the case without considering airflow cooling (Fig. 7(a)). The

numerical simulation shows that radial ventilation plays a very significant role in cooling of the disk in the braking phase. The higher convection coefficients achieved by airflow cooling will not only reduce the maximum temperature at the friction interface, but also naturally tend to reduce thermal gradients of the cooling ribs and the parts where the disk are bolted to the hub, since heat will be removed faster from hotter parts of the disk. So the airflow cooling should be very effective to reduce the risk of MHS formation.

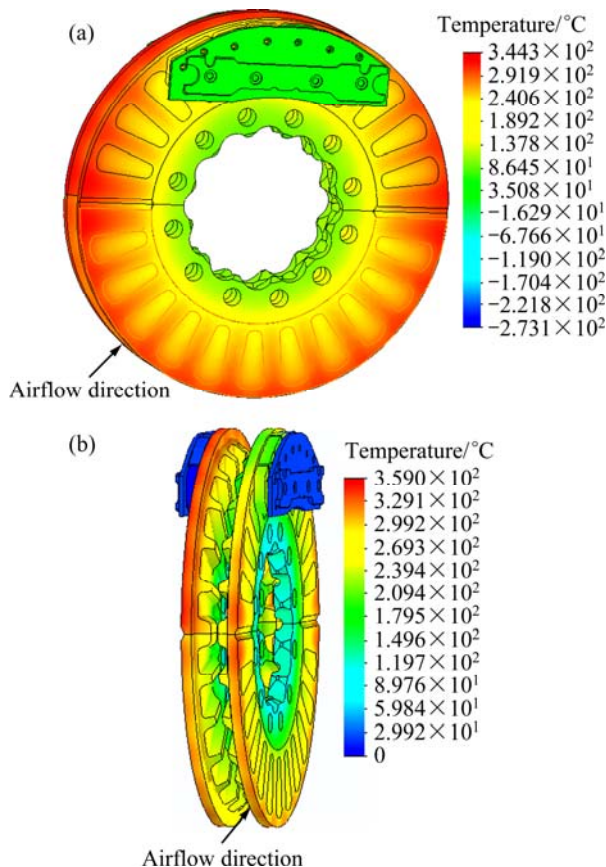


Fig. 9 Numerical simulation of temperature of SiC_n/6061 brake disk considering airflow cooling: (a) Temperature distribution of friction interface; (b) Temperature distribution from side elevation direction

4.3.2 Analysis of stress

Figure 10(a) shows that cooling ribs play a very significant role in cooling of the disk in the braking stage considering airflow cooling. The variation of non-dimensional radial thermal stress is due to thermo mechanical load of the mounted SiC_n/6061 brake disks with different values of the temperature gradient. This phenomenon can be explained by the presence of interactive effects between thermomechanical load and contact area. It is seen that the maximum thermal radial stress decreases to 164 MPa, which is lower than 269 MPa as shown in Fig. 8(b). Thermal stress distribution of friction interface is not centrosymmetry and the thermal

stress course has a curved elliptical shape as a result of airflow cooling.

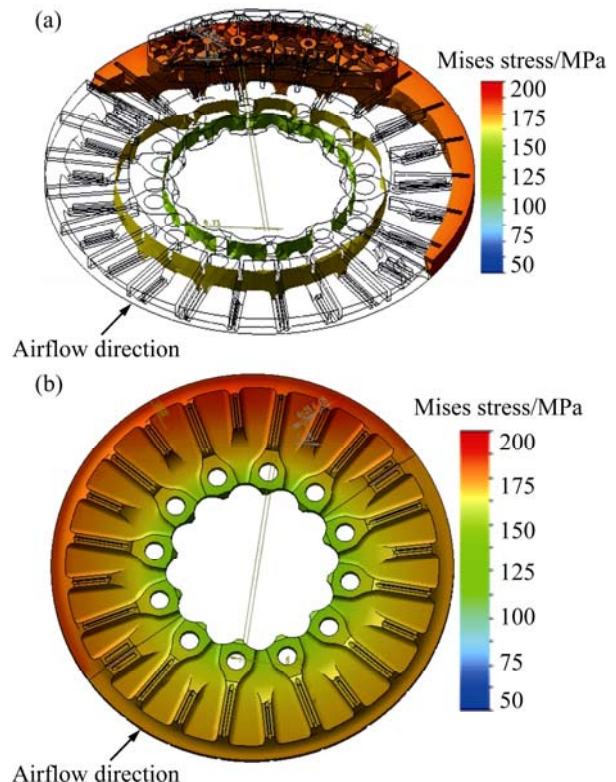


Fig. 10 Numerical simulation of thermal stress of SiC_n/6061 brake disk with considering airflow cooling: (a) Thermal stress distribution of friction interface; (b) Thermal stress distribution from back elevation direction

4.4 Comparison of experiment results with simulation considering airflow cooling

The dry friction and wear behavior of 6061 Al alloy reinforced with SiC continuous ceramic network against Cu alloy reinforced with SiC continuous ceramic network were studied with the MM1000-type ring-on-ring wear tester under the condition of emergency braking at the speed of 300 km/h considering airflow cooling at room temperature. The detail of the test was illustrated in Ref. [31]. In our experiment, the rings made of SiC_n/6061 and SiC_n/Cu after the test were usually destroyed, cracked and overheated. Figure 11 shows that the temperature at the friction interface increases at first, and then decreases; the highest temperature by simulation is lower than the experimental data. It can be seen that the experimental results are very similar to those obtained by numerical simulation. It is observed that the temperature obtained by simulation reaches the maximum of 461 °C at 107 s while the experimental data comes up to the maximum of 532 °C at 93 s without considering airflow cool. However, the simulated temperature reaches the maximum of 359 °C at 105 s, while the experimental data reach up to 392 °C at 98 s considering airflow cooling. The measured

cooling curves in 50–200 °C are superimposed on the predicted curve, showing its accuracy based on CFD coupled heat calculation method. The agreement between the measured and predicted values at lower temperatures is good. It shows that airflow cooling can remove heat from the brake disc rapidly. The predicted temperature is lower than the measured in the range of 300–500 °C, which can be explained that there is a large delay or time lag for brake disc's temperature as measured in our experiment, no cooling occurred at the beginning of the braking. Therefore the surface temperature increases sharply at this time, thus the aerodynamic design has inconsiderable effect on the reduction of maximum temperature at the braking surface [31]. And higher convection coefficient might influence the heating of the disc during braking itself. The simulated results of the braking are similar to those of MARTIN et al [32]. Additionally, the distance of airflow from the edge of the disk [33], the airflow direction [34], and the radial locations of around r/D [35], were not considered in the simulation, which might influence the cooling of the disc.

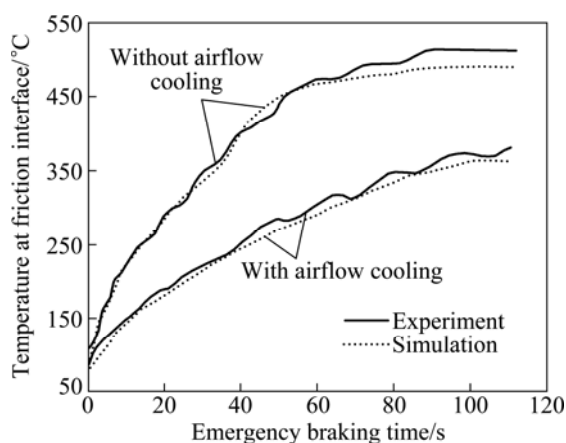


Fig. 11 Measured and predicted temperature at friction surface of $\text{SiC}_n/6061$ brake disk during emergency braking with or without considering airflow cooling

5 Conclusions

The thermal and stress analyses of a $\text{SiC}_n/6061$ composite brake disk for CRH3 railway vehicles during emergency braking at a speed of 300 km/h with and without considering the airflow cooling were studied using FE and CFD methods. The results revealed that $\text{SiC}_n/6061$ composite can effectively enhance the thermal performance of the brake disk; the highest temperature after emergency braking was 461 °C and 359 °C without and with considering airflow cooling, which occurred at about 107 s and 105 s, respectively. The maximum stress can reach 269 MPa and 164 MPa without and with considering airflow cooling, respectively. The $\text{SiC}_n/6061$

composite will not only reduce the maximum temperature, but also naturally tend to reduce the thermal gradients. $\text{SiC}_n/6061$ composite and airflow cooling should therefore be very effective to reduce the risk of MHS formation. The measured cooling curves are superimposed on the predicted curve to show its accuracy based on our CFD coupled heat calculation method.

References

- [1] DAOUD A, ABOUEL-KHAIR M T. Wear and friction behavior of sand cast brake rotor made of A359-20vol%SiC particle composites sliding against automobile friction material [J]. *Tribology International*, 2010, 43: 544–553.
- [2] SKIRL S, HOFFMAN M, BOWMAN K, WIEDERHORN S, RODEL J. Thermal expansion behavior and macrostrain of 3D-SiC/Al composites with interpenetrating networks [J]. *Acta Mater*, 1998, 46(7): 2493–2499.
- [3] HOFFMAN M, SKIRL S, POMPE W, RODEL J. Thermal residual strains and stresses in 3D-SiC/Al composites with interpenetrating networks [J]. *Acta Mater*, 1999, 47(2): 565–577.
- [4] LU S K, LIU H Y, YU L, JIANG Y L. 3D FEM simulations for the homogeneity of plastic deformation in aluminum alloy HS6061-T6 during ECAP [J]. *Procedia Engineering*, 2011, 12: 35–40.
- [5] YU Liang, JIANG Yan-li, LU Sen-kai, RU Hong-qiang, FANG Ming. FEM for brake discs of SiC 3D continuous ceramic reinforced 7075 aluminum alloy for CRH3 trains applying emergency braking [J]. *Applied Mechanics and Materials*, 2012, 120: 51–55.
- [6] YU Liang, JIANG Yan-Li, LU Sen-kai, LUO Kun, RU Hong-qiang. Numerical simulation of brake discs of CRH3 high-speed trains based on Ansys [C]//ALLISON J, COLLINS P, SPANOS G. *Proceedings of the 1st World Congress on Integrated Computational Materials Engineering (ICME)*. Hoboken, NJ, USA: John Wiley & Sons, Inc, 2011: 183–188. DOI: 10.1002/9781118147726.ch25
- [7] ODER G, REIBENSCHUH M, LERHER T, SRAML M, SAMEC B, POTRC I. Thermal and stress analysis of brake disks in railway vehicles [J]. *Advanced Engineering*, 2009, 3(1): 95–102.
- [8] ZHANG C Q, ZHANG L T, ZENG Q F, FAN S W, CHENG L F. Simulated three-dimensional transient temperature field during aircraft braking for C/SiC composite brake disc [J]. *Materials & Design*, 2011, 32(5): 2590–2595.
- [9] ZHU Zhen-cai, PENG Yu-xing, SHI Zhi-yuan, CHEN Guo-an. Three-dimensional transient temperature field of brake shoe during hoist's emergency braking [J]. *Applied Thermal Engineering*, 2009, 29(5–6): 932–937.
- [10] PEVEC M, LERHER T, POTRC I, VRANEŠEVIĆ D. Numerical temperature analysis of brake disk considering cooling [J]. *Advanced Engineering*, 2010, 4(1): 55–64.
- [11] MACKIN T J, NOE S C, BALL K J. Thermal cracking in disc brakes [J]. *Engineering Failure Analysis*, 2002, 9(1): 63–67.
- [12] YANG Y, ZHOU J M. Numerical simulation study of 3-D thermal stress field with complex boundary [J]. *Journal of Engineering Thermophysics*, 2007, 27(3): 487–489.
- [13] SHAHZAMANIAN M M, SAHARI B B, BAYAT M, MUSTAPHA F, ISMARRUBIE Z N. Finite element analysis of thermoelastic contact problem in functionally graded axisymmetric brake disks [J]. *Composite Structures*, 2010, 22: 1591–1602.
- [14] PENG Yu-xing, ZHU Zhen-cai, CHEN Guo-an, BAO Jiu-sheng, LIU Bin-bin, LI Yi-lei. Temperature field of disk brake for mine hoist [J]. *Advanced Science Letters*, 2011, 4(6–7): 2380–2385.

- [15] KOLHE R, HUI C Y, USTUNDAG E, SASS S L. Residual thermal stresses and calculation of the critical metal particle size for interfacial crack extension in metal–ceramic matrix composites [J]. *Acta Mater*, 1996, 44(1): 279–287.
- [16] YILDIZ Y, DUZGUN M. Stress analysis of ventilated brake disks using the finite element method, international [J]. *Journal of Automotive Technology*, 2010, 11(1): 133–138.
- [17] YANG Y C, WEN L C. A nonlinear inverse problem in estimating the heat flux of the disk in a disk brake system [J]. *Applied Thermal Engineering*, 2011, 31: 2439–2448.
- [18] ADAMOWICZ A, GRZES P. Influence of convective cooling on a disk brake temperature distribution during repetitive braking [J]. *Applied Thermal Engineering*, 2011, 31(14–15): 2177–2185.
- [19] LU S K, SU J H, LIAO S D, SU J Q, WANG B, YU L, JIANG Y L, WEN S H. Finite element analysis on fatigue failure prediction of a rear axle housing of vehicle based on Cosmos [J]. *Applied Mechanics and Materials*, 2012, 121–126: 843–847.
- [20] YU Liang, JIANG Yan-li, RU Hong-qiang, LIU Jiang-tao, LUO Kun. Microstructures of co-continuous SiC/Fe-2Cr13 composite fabricated by vacuum-pressure casting and infiltration processes [J]. *Advanced Materials Research*, 2011, 239–242: 1661–1664.
- [21] YEVTUSHENKO A, IVANYK E. Determination of temperatures for sliding contact with applications for braking systems [J]. *Wear*, 1997, 206(1–2): 53–59.
- [22] AGRAWAL P, CONLON K, BOWMAN K J, SUN C T, CICHOCKI F R Jr, TRUMBLE K P. Thermal residual stresses in co-continuous composites [J]. *Acta Materialia*, 2003, 51: 1143–1156.
- [23] AFFERRANTE L, CIAVARELLA M, DECUZZI P, DEMELIO G. Transient analysis of frictionally excited thermoelastic instability in multi-disk clutches and brakes [J]. *Wear*, 2003, 254(1–2): 136–146.
- [24] LYONES O F P, MURRAY D B, TORRANCE A A. Air jet cooling of brake discs [J]. *IMEchE Proceedings*, 2008, 222(6): 995–1004.
- [25] VOLDRICH J. Frictionally excited thermoelastic instability in disc brakes-transient problem in the full contact regime [J]. *International Journal of Mechanical Sciences*, 2007, 49(2): 129–137.
- [26] CHOI J H, LEE I. Finite element analysis of transient thermoelastic behaviors in disk brakes [J]. *Wear*, 2004, 257(1–2): 47–58.
- [27] MARKO T. Energy thrift and improved performance achieved through novel railway brake discs [J]. *Applied Energy*, 2009, 86: 317–324.
- [28] GALINDO-LOPEZ C H, TIROVIC M. Understanding and improving the convective cooling of brake disc with radial vanes [J]. *Journal of Automobile Engineering*, 2008, 222(7): 1211–1229.
- [29] THURESSON D. Stability of sliding contact-comparison of a pin and a finite element model [J]. *Wear*, 2006, 261(7–8): 896–904.
- [30] QI H S, DAY A J. Investigation of disc/pad interface temperatures in friction braking [J]. *Wear*, 2007, 262(5–6): 505–513.
- [31] BAYDAR E, OZMEN Y. An experimental and numerical investigation on a confined impinging air jet at high Reynolds numbers [J]. *Applied Thermal Engineering*, 2005, 25(2–3): 409–421.
- [32] MARTIN H. Heat and mass transfer between impinging gas jets and solid surfaces, *Advances in heat transfer* [M]. Volume 13. New York: Academic Press, Inc., 1977: 1–60.
- [33] O'DONOVAN T S, MURRAY D B. Jet impingement heat transfer – part I: Mean and rootmean-square heat transfer and velocity distributions [J]. *International Journal of Heat and Mass Transfer*, 2007, 50: 3291–3301.
- [34] HUANG L, EL-GENK M S. Heat transfer of an impinging jet on a flat surface [J]. *International Journal of Heat and Mass Transfer*, 1994, 37: 1915–1923.
- [35] BAUGHN J W, SHIMIZU S S. Heat transfer measurements from a surface with uniform heat flux and an impinging jet [J]. *ASME Journal of Heat Transfer*, 1989, 111: 1096–1098.

用于 CRH3 的 SiC/6061 铝合金共连续复合材料制动盘在紧急制动过程中考虑气流冷却情况下的热分析

姜 澜¹, 姜艳丽², 喻 亮², 苏 楠¹, 丁友东¹

1. 东北大学 材料与冶金学院, 沈阳 110819;

2. 桂林理工大学 有色金属及材料加工新技术教育部重点实验室, 桂林 543004

摘 要: 使用 SiC 网络陶瓷骨架增强的 6061 铝合金复合材料(SiC_n/Al)制动盘可以减少高速列车的质量。采用有限元(FE)和计算流体动力学(CFD)方法计算在 300 km/h 速度下实施紧急制动过程中考虑气流冷却条件下 SiC_n/Al 制动盘的热和应力。分析制动器总成及其界面的设计特点时考虑了传导、对流和辐射这三种传热的模式。结果表明, 具有较高对流系数的气流冷却不仅降低制动中的最高温度, 也降低了温度梯度, 因为气流加速了制动盘上较热部分的热量散失。有效的气流冷却可以减少制动盘上热斑的形成和盘体的热变形。有无考虑气流冷却时, 实施紧急制动后, 制动盘最高温度分别为 461 ℃和 359 ℃。有无考虑气流冷却时, 制动盘的等效压力可分别达到 269 和 164 MPa。然而, 在实施紧急制动时, 制动盘表面的最大应力可能超过材料的屈服强度, 这可能导致在不带冷却时制动盘的塑性损伤累积。模拟结果与实验结果相一致。

关键词: 有限元法; 制动盘; 共连续 SiC/6061 复合材料; 热分析; 气流冷却

(Edited by YUAN Sai-qian)